

## COOLING TIMESCALES AND TEMPORAL STRUCTURE OF GAMMA-RAY BURSTS

RE'EM SARI

Racah Institute for Physics, The Hebrew University, Jerusalem 91904, Israel

RAMESH NARAYAN

Harvard-Smithsonian Center for Astrophysics, 60 Garden Street, Cambridge MA 02138

AND

TSVI PIRAN

Racah Institute for Physics, The Hebrew University, Jerusalem 91904, Israel

*Received 1996 April 30; accepted 1996 June 26*

### ABSTRACT

A leading mechanism for producing cosmological gamma-ray bursts (GRBs) is via ultrarelativistic particles in an expanding fireball. The kinetic energy of the particles is converted into thermal energy in two shocks, a forward shock and a reverse shock, when the outward flowing particles encounter the interstellar medium. The thermal energy is then radiated via synchrotron emission and Comptonization. We estimate the synchrotron cooling timescale of the shocked material in the forward and reverse shocks for electrons of various Lorentz factors, focusing in particular on those electrons whose radiation falls within the energy detection range of the BATSE detectors. We find that in order to produce the rapid variability observed in most bursts, the energy density of the magnetic field in the shocked material must be greater than about 1% of the thermal energy density. In addition, the electrons must be nearly in equipartition with the protons, since otherwise we do not have reasonable radiative efficiencies of GRBs. Inverse Compton scattering can increase the cooling rate of the relevant electrons, but the Comptonized emission itself is never within the BATSE range. These arguments allow us to pinpoint the conditions within the radiating regions in GRBs and to determine the important radiation processes. In addition, they provide a plausible explanation for several observations. The model predicts that the duty cycle of intensity variations in GRB light curves should be nearly independent of burst duration and should scale inversely as the square root of the observed photon energy. Both correlations are in agreement with observations. The model also provides a plausible explanation for the bimodal distribution of burst durations. There is no explanation, however, for the presence of a characteristic break energy in GRB spectra.

*Subject headings:* gamma rays: bursts — hydrodynamics — radiation mechanisms: nonthermal — relativity — shock waves

### 1. INTRODUCTION

A cosmological gamma-ray burst (GRB) occurs, most likely in the deceleration of a shell of ultrarelativistic particles encountering a surrounding interstellar medium (ISM) (Mészáros & Rees 1992). This process is believed to be essential for the production of a GRB regardless of the specific nature of the original source of relativistic particles (see, e.g., Piran 1995 for a discussion). In a recent paper, Sari, & Piran (1995, hereafter SP) estimated the hydrodynamical timescales that arise in the interaction of an ultrarelativistic shell with the ISM. They showed that the observed durations of GRBs impose a direct limit on the Lorentz factors of the relativistic particles, namely,  $\gamma > 100$  for most bursts and  $\gamma$  even larger in a few cases. SP also worked out the hydrodynamical conditions in the various fluid zones of the expanding shell. They calculated the bulk velocity, thermal energy, and particle density in the shocked material behind the forward and reverse shocks, as well as the velocities of the two shock fronts.

The radiation we observe in a GRB is produced when the shock-heated gas loses its thermal energy through various radiation processes. In this paper, we consider the cooling of the shocked material via synchrotron and inverse Compton emission.

In developing a radiation model for GRBs, we can consider two distinct possibilities, depending on the relative

magnitudes of the cooling timescale of the thermal electrons,  $t_{\text{cool}}$ , and the hydrodynamical timescale of the expanding shell,  $t_{\text{hyd}}$ . The case we focus on in this paper is similar to that assumed by SP, namely, that  $t_{\text{hyd}} > t_{\text{cool}}$ . This assumption finds strong support in the fact that most bursts have complicated temporal structure with multiple peaks. A natural explanation is that the total duration of a burst is due to  $t_{\text{hyd}}$ , the time needed to convert the bulk of the kinetic energy of the expanding shell into thermal energy via the two shocks, while the individual peaks within the profile arise because of shotlike thermalization events in the shocks. In this picture, the individual subpeaks within a burst represent the cooling curves of episodically heated electrons. The width of an individual subpeak then represents the cooling timescale  $t_{\text{cool}}$ , and the “duty cycle” of the burst, which we define to be the ratio of the observed width of an individual peak to the total duration of the burst, is given by the ratio  $D = t_{\text{cool}}/t_{\text{hyd}}$ .

The second case, which we do not consider in this paper, is when  $t_{\text{hyd}} < t_{\text{cool}}$ . Here the kinetic energy of the expanding shell is turned rapidly into thermal energy, but it is then released as radiation on a slower timescale. Clearly, this regime can lead only to smooth single-hump bursts. Since most bursts have multiple subpeaks, it is necessary to identify each peak with a single hump, which means that  $t_{\text{hyd}}$  must be smaller than the width of a subpeak. But such short

$t_{\text{hyd}}$  requires extremely high Lorentz factors (SP). In addition, a new mechanism is needed to explain the overall duration of the burst.

In addition to the assumption  $t_{\text{hyd}} > t_{\text{cool}}$ , we make the further assumption that the hydrodynamical conditions do not change significantly during the cooling of the electrons. In other words, we assume that the rapid cooling does not modify drastically the adiabatic shock structure calculated by SP. This is a reasonable approximation if the thermalization in the shocks transfers half or more of the energy to the protons and only the remainder to the electrons. While the electrons cool rapidly, the proton energy remains locked up in the gas, leaving the hydrodynamical conditions relatively unaffected. The true conditions will thus differ from the idealized adiabatic shocks considered by SP by only factors of order unity, which we ignore.

In this paper, we use two pieces of information from observations to constrain the parameters of our model of the radiating regions of GRBs. First, we note that the vast majority of GRBs have complex time profiles in which individual subpeaks are significantly narrower than the overall duration of a burst. Roughly, the observations give a mean duty cycle of about 5%. As we show, this provides a significant constraint on the model. Second, we demand efficient conversion of thermal energy into radiation at the two shocks, since we feel that low-efficiency burst models are implausible. The observations show that the net energy emitted by cosmological bursts just within the BATSE band is  $\sim 10^{51}$  ergs (Cohen & Piran 1995; Fenimore et al. 1993). In the most popular models of bursts, namely, merging neutron star binaries (Narayan, Paczyński, & Piran 1992) and failed supernovae (Woosley 1993), the total energy budget is only  $\sim 10^{53.3}$  ergs, and there are some difficulties in converting even 1% of the initial explosion energy into kinetic energy of the expanding shell. Any further inefficiency in the conversion of shock thermal energy into radiation would be catastrophic.

We show in this paper that to produce the rapid variability observed in many bursts, the magnetic energy density in the shocked region must be at least 1% of the random thermal energy density of the gas. In addition, we show that in order to have a reasonable radiative efficiency, the electrons must be nearly in equipartition with the protons. Thus, the observational data on GRBs restrict directly the conditions in the emitting region of these sources.

We ignore the time spreading due to the curvature of the emitting region (Katz 1994) and therefore obtain only an upper limit on the observed variability. In addition, we base our calculations on the simple assumption of homogeneous ISM. The time spreading due to the source curvature may require to ease this assumption.

We begin the paper with a brief summary in § 2 of the main results from SP, namely, the hydrodynamical timescale of the shell and the characteristics of the forward and reverse shocks. We continue with an estimate of the synchrotron cooling timescale in § 3, and we establish a lower limit for the magnetic field strength in the shocked material. In § 4 we examine the role of inverse Compton (IC) emission. We show that this process is irrelevant in the forward shock, since the electrons there are too energetic and the scattering cross section is reduced considerably according to the Klein-Nishina formula. IC can be important in the reverse shock and can increase the cooling rate there. However, the IC photons themselves will in general be

outside the energy range of the BATSE detector and therefore are not relevant for understanding the BATSE data.

In § 5 we discuss the distribution of electron energy and the effect this has on the “efficiency” of a burst, namely, the fraction of the initial kinetic energy in the shell that finally appears as radiation in the BATSE energy window. We show that the forward shock often produces nearly all its radiation at energies above the BATSE range, especially for short duration bursts. In contrast, the reverse shock is always visible to BATSE. However, the efficiency of the reverse shock is usually somewhat low, whereas the forward shock, when it radiates within the BATSE window, always has a high efficiency. We show in § 6 that these characteristics of the two shocks provide a plausible explanation for the bimodal distribution of GRB durations observed by BATSE (Kouveliotou et al. 1993; Lamb, Graziani, & Smith 1993). We suggest that short bursts originate from the reverse shocks of fireballs that expand with high Lorentz factor  $\gamma$ , while long bursts originate from the forward shock of low  $\gamma$  events. This simple model is also in agreement with the relative luminosities of short and long bursts as estimated by Mao, Narayan, & Piran (1994).

## 2. SHOCK CONDITIONS AND HYDRODYNAMIC TIMESCALES

We begin with a brief summary of the hydrodynamic conditions and energy conversion timescales of a relativistically expanding shell of particles, treated as a fluid (see SP and Piran 1995 for further details). The interaction between the outward moving shell and the ISM takes place in the form of two shocks: a forward shock that propagates into the ISM and a reverse shock that propagates into the relativistic shell. This results in four distinct regions: the ISM at rest (denoted by the subscript 1 when we consider properties in this region), the shocked ISM material that has passed through the forward shock (subscript 2 or  $f$ ), the shocked shell material that has passed through the reverse shock (3 or  $r$ ), and the unshocked material in the shell (4).

See Figure 1.

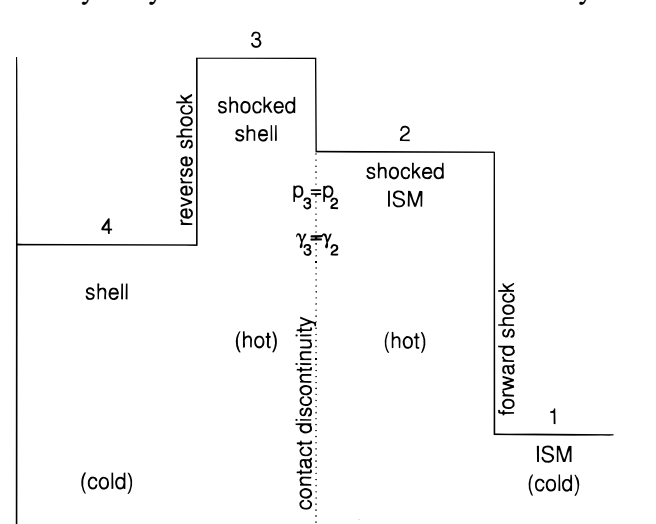


FIG. 1.—Schematic representation of the four zones that are present when a relativistic fireball interacts with the ISM. The solid line indicates the density as a function of radius. The undisturbed ISM is zone 1 at large radius, and the unshocked shell material is zone 4 at small radii. The shocked zones, 2 and 3, are the result of the forward and reverse shocks and are separated by a contact discontinuity (based on Sari & Piran 1995).

parameters: the Lorentz factor  $\gamma$  associated with the relativistic radial expansion of the shell of particles, the width of the shell in the observer frame  $\Delta$ , the density of the external ISM  $n_1$ , and the Sedov scale  $l = (E/n_1 m_p c^2)$ , where  $E$  represents the total energy of the shell before interaction with the ISM. Typical values of these parameters are  $\gamma \sim 10^2 - 10^4$ ,  $\Delta < 10^{13}$  cm (from the fact that bursts are almost always less than a few hundred seconds long; see SP),  $n_1 = 1$  particle per  $\text{cm}^{-3}$ , and  $l = 10^{18}$  cm (corresponding to a burst with energy  $E = 1.5 \times 10^{51}$  ergs).

The radial expansion speeds of the four zones are described by the following Lorentz factors. The unshocked ISM is of course at rest and has  $\gamma_1 = 1$ , while the unshocked shell material moves at the original coasting velocity of the particles,  $\gamma_4 = \gamma$ . The velocity of the two intermediate zones satisfies  $\gamma_1 < \gamma_2 = \gamma_3 < \gamma_4$ . The relative Lorentz factor across the forward shock is obviously equal to  $\gamma_2$ . The relative Lorentz factor across the reverse shock, which we write as  $\bar{\gamma}_3$ , is given in the ultrarelativistic limit by

$$\bar{\gamma}_3 = \gamma/\gamma_3, \quad (1)$$

where we have ignored, as in the rest of the paper, factors of order unity.

SP showed that the structure of the shocks depends on the value of  $\bar{\gamma}_3$ , which in turn depends on the parameter  $\xi$ :

$$\xi \equiv \left(\frac{l}{\Delta}\right)^{1/2} \gamma^{-4/3}. \quad (2)$$

If  $\xi \gg 1$ , the reverse shock is nonrelativistic or Newtonian, and  $\bar{\gamma}_3 \sim 1$ , while if  $\xi \ll 1$  the reverse shock is relativistic and  $\bar{\gamma}_3 \gg 1$ . If we include the possibility of shell spreading (see SP for details), then  $\Delta$  changes with time in such a manner that at each moment the current  $\Delta(t) \sim \max[\Delta(0), R/\gamma^2]$ . This means that a shell that begins with a value of  $\xi > 1$  adjusts itself so as to satisfy  $\xi = 1$ , and we have a mildly relativistic or Newtonian reverse shock, whereas a shell with  $\xi < 1$  does not have time to spread significantly and maintains a relativistic reverse shock. In the rest of the paper, we concentrate on the relativistic case and express all results in terms of the parameter  $\xi$  (rather than  $\Delta$ ). By setting  $\xi < 1$  in the expressions, we obtain results corresponding to a relativistic reverse shock, and by choosing  $\xi = 1$  in the same expressions we obtain the spreading Newtonian limit. We will not discuss the case of extreme Newtonian reverse shock ( $\xi \gg 1$ ), since spreading will always bring these shells to the mildly relativistic limit ( $\xi \sim 1$ ), which we call ‘‘Newtonian’’ in the rest of the paper. Therefore, the same formulae are valid in both the relativistic and Newtonian limits.

According to the arguments presented in the Introduction, the observed duration  $t_{\text{dur}}$  of a burst is given by the hydrodynamic time  $t_{\text{hyd}}$  of the shell which has been calculated by SP to be

$$t_{\text{dur}} = \left(\frac{l}{c}\right) \gamma^{-8/3} \xi^{-2} = (150 \text{ s}) \left(\frac{\gamma}{100}\right)^{-8/3} \xi^{-2} l_{18}, \quad (3)$$

where  $l_{18} = l/10^{18}$  cm. This timescale is equal to  $\Delta/c$  in both the relativistic and Newtonian cases, except that in the former case the width is independent of the radius of the shell, whereas in the latter the width expands self-consistently so as to maintain  $\xi = 1$ .

The bulk of the kinetic energy of the shell is converted to thermal energy via the two shocks at around the time the

shell has expanded to the radius  $R_\Delta \equiv l \gamma^{-2/3} \xi^{-1/2}$ . At this radius, the conditions at the forward shock are as follows:

$$\begin{aligned} \gamma_2 &= \gamma \xi^{3/4}, \\ n_2 &= 4\gamma_2 n_1, \\ e_2 &= 4\gamma_2^2 n_1 m_p c^2, \end{aligned} \quad (4)$$

while at the reverse shock we have

$$\begin{aligned} \bar{\gamma}_3 &= \xi^{-3/4}, \\ \gamma_3 &= \gamma \xi^{3/4}, \\ n_3 &= 4\xi^{9/4} \gamma^2 n_1, \\ e_3 &= e_2. \end{aligned} \quad (5)$$

We see from equation (3) that the observed duration of a burst depends on  $\gamma$  and  $\xi$  only through the combination  $\gamma_2 = \gamma \xi^{3/4}$ . Therefore, many observed quantities that depend on  $\gamma_2$  can be expressed in terms of  $t_{\text{dur}}$  via the relation (see eqs. [3] and [4])

$$\gamma_2 = 280 \left(\frac{t_{\text{dur}}}{10 \text{ s}}\right)^{-3/8} l_{18}^{3/8}. \quad (6)$$

The efficiency of the cooling processes and the nature of the emitted radiation depend on the conditions in the shocked regions 2 and 3. Both regions have the same energy density  $e$ . The particle densities  $n_2$  and  $n_3$  are, however, different, and hence the effective ‘‘temperatures,’’ i.e., the mean Lorentz factors of the random motions of the shocked protons and electrons, are different. The parameters that determine the radiative cooling are the magnetic field strength,  $B$ , and the distribution of electron Lorentz factor  $\gamma_e$ . Both of these are difficult to estimate from first principles. Our approach is to use two parameters,  $\epsilon_B$  and  $\epsilon_e$  defined below, to incorporate our uncertainties. Then we explore the space of these parameters and try to constrain the parameter values by requiring the model predictions to resemble BATSE observations of GRBs.

The dimensionless parameter  $\epsilon_B$  measures the ratio of the magnetic field energy density to the total thermal energy  $e$ :

$$\epsilon_B \equiv \frac{U_B}{e} = \frac{B^2}{8\pi e}, \quad (7)$$

so that

$$B = 4\sqrt{2\pi c \epsilon_B^{1/2} \gamma_2 m_p^{1/2} n_1^{1/2}} = (110 \text{ G}) \epsilon_B^{1/2} \left(\frac{t_{\text{dur}}}{10 \text{ s}}\right)^{-3/8} l_{18}^{3/8} n_1^{1/2}. \quad (8)$$

If the magnetic field in region 2 behind the forward shock is obtained purely by shock compression of the ISM field, the field would be very weak, with  $\epsilon_B \ll 1$ . Such low fields are incompatible with observations of GRBs as we show in later sections. Therefore, we consider the possibility that there may be some kind of a turbulent instability that may bring the magnetic field to approximate equipartition. In the case of the reverse shock, magnetic fields of considerable strength might be present in the preshock shell material if the original exploding fireball was magnetic. The exact nature of magnetic field evolution during fireball expansion depends on several assumptions. Thompson (1994) found that the magnetic field will remain in equipartition if it

started off originally in equipartition. Mészáros, Laguna, & Rees (1993), on the other hand, estimated that if the magnetic field was initially in equipartition, then it would be below equipartition by a factor of  $10^{-5}$  by the time the shell expands to  $R_A$ . As in the forward shock, an instability could boost the field back to equipartition. Thus, while both shocks may have  $\epsilon_B \ll 1$  with pure flux freezing, both could achieve  $\epsilon_B \rightarrow 1$  in the presence of instabilities. In principle,  $\epsilon_B$  could be different for the two shocks, but we limit ourselves to the same  $\epsilon_B$  in both shocks.

Our second parameter  $\epsilon_e$  measures the fraction of the total thermal energy  $e$  that goes into random motions of the electrons:

$$\epsilon_e \equiv \frac{U_e}{e}. \quad (9)$$

We assume that the thermal energy immediately behind the shock is divided up in the ratio  $(1 - \epsilon_e)$ :  $\epsilon_e$  between the protons and the electrons. We assume that the division happens on a timescale that is shorter than the electron cooling time, and therefore much shorter than the hydrodynamic time. We assume further that once the initial allocation of the energy has been accomplished, no further energy flows to the electrons from the protons. (It is easily seen that Coulomb coupling is completely negligible at the densities of interest.)

Since the electrons receive their random motions through shock heating, we make the standard assumption that they develop a power-law distribution of Lorentz factors,

$$N(\gamma_e) \sim \gamma_e^{\bar{\beta}} \quad \text{for } \gamma_e > \gamma_{e,\min}. \quad (10)$$

We require  $\bar{\beta} < -2$  so that the energy does not diverge at large  $\gamma_e$ . Since our shocks are relativistic, we assume that all the electrons participate in the power law, not just a small fraction in the tail of the distribution as in the Newtonian case. The minimum Lorentz factor,  $\gamma_{e,\min}$ , of the distribution is related to  $\epsilon_e$  by

$$\epsilon_e e = \gamma_{e,\min} n m_e c^2 \frac{\bar{\beta} + 1}{\bar{\beta} + 2}, \quad e \sim \gamma_{\text{sh}} n m_p c^2, \quad (11)$$

where  $\gamma_{\text{sh}}$  is the relative Lorentz factor across the shock front. Thus,

$$\gamma_{e,\min} = 1840 \frac{(\bar{\beta} + 2)}{(\bar{\beta} + 1)} \epsilon_e \gamma_{\text{sh}}. \quad (12)$$

The average  $\gamma_e$  of the electrons is given by

$$\langle \gamma_e \rangle = \frac{(\bar{\beta} + 1)}{(\bar{\beta} + 2)} \gamma_{e,\min}. \quad (13)$$

Note that  $\gamma_{\text{sh}} = \gamma_2$  for the forward shock and  $\gamma_{\text{sh}} = \bar{\gamma}_3$  for the reverse shock.

The energy index  $\bar{\beta}$  can be fixed by requiring that the model should be able to explain the high-energy spectra of GRBs. If we assume that most of the radiation observed in the BATSE window is due to synchrotron cooling (as we confirm later in the paper), then it is straightforward to relate  $\bar{\beta}$  to the power-law index of the observed spectra of GRBs. Band et al. (1993) measured the mean spectral index of GRBs at high photon energies (above the break) to be  $\beta \approx -2.25$ , which corresponds to  $\bar{\beta} \approx -2.5$ . We assume

this value of  $\bar{\beta}$  in what follows:

$$\bar{\beta} = -2.5, \quad \frac{(\bar{\beta} + 1)}{(\bar{\beta} + 2)} = 3. \quad (14)$$

The electrons in zone 2 behind the forward shock then satisfy

$$\gamma_{e,\min} = \frac{1}{3} \langle \gamma_e \rangle = 610 \epsilon_e \gamma_2 = 1.7 \times 10^5 \epsilon_e \left( \frac{t_{\text{dur}}}{10 \text{ s}} \right)^{-3/8} l_{18}^{3/8}, \quad (15)$$

while the electrons in zone 3 behind the reverse shock have

$$\gamma_{e,\min} = \frac{1}{3} \langle \gamma_e \rangle = 610 \epsilon_e \xi^{-3/4}. \quad (16)$$

We shall see later that the precise details of the distribution of  $\gamma_e$  are not very important for most of the calculations presented in this paper; only the value of  $\gamma_{e,\min}$  is relevant.

### 3. SYNCHROTRON COOLING

The typical energy of synchrotron photons as well as the synchrotron cooling time depend on the Lorentz factor  $\gamma_e$  of the relativistic electrons under consideration and on the strength of the magnetic field. The characteristic photon energy in the fluid frame is given by

$$(h\nu_{\text{syn}})_{\text{fluid}} = \frac{\hbar q_e B}{m_e c} \gamma_e^2. \quad (17)$$

Since the emitting material in both shocks moves with a Lorentz factor  $\gamma_2$ , the photons are blueshifted in the observer frame:

$$(h\nu_{\text{syn}})_{\text{obs}} = \frac{\hbar q_e B}{m_e c} \gamma_e^2 \gamma_2 = (3.5 \times 10^{-7} \text{ keV}) \times \gamma_e^2 \epsilon_b^{1/2} \left( \frac{t_{\text{dur}}}{10 \text{ s}} \right)^{-3/4} l_{18}^{3/4} n_1^{1/2}. \quad (18)$$

The power emitted by a single electron due to synchrotron radiation (see, e.g., Rybicki & Lightman 1979) is

$$P = \frac{4}{3} \sigma_T c U_B \gamma_e^2, \quad (19)$$

where  $\sigma_T$  is the Thomson cross section. The cooling time of the electron in the fluid frame is then  $\gamma_e m_e c^2 / P$ . The observed cooling time  $\tau_{\text{syn}}$  is shorter by a factor of  $\gamma_2$ , giving

$$\tau_{\text{syn}} = \frac{3 \gamma_e m_e c^2}{4 \sigma_T c U_B \gamma_e^2 \gamma_2} = (230 \text{ s}) \frac{1}{\gamma_e} \epsilon_B^{-1} \left( \frac{t_{\text{dur}}}{10 \text{ s}} \right)^{9/8} l_{18}^{-9/8} n_1^{-1}. \quad (20)$$

The above results depend on the choice of  $\gamma_e$ . One possibility (following Mészáros et al. 1993) is to consider the Lorentz factor of a “typical electron” in the emitting region, i.e., to set  $\gamma_e = \langle \gamma_e \rangle$ , and to use this for estimating the cooling timescale. However, it is not clear that the photons emitted by such electrons will actually be within BATSE’s range. Since BATSE detects photons with energies  $\sim 100$  keV, we concentrate on electrons with Lorentz factor  $\hat{\gamma}_e$ , where  $\hat{\gamma}_e$  is that Lorentz factor at which an electron emits synchrotron photons with energies around  $\sim 100$  keV. Of course other electrons are also present in the medium. But the electrons with lower energies emit softer

photons, while the higher energy electrons emit harder photons that fall outside the BATSE range (but may be detected by other experiments which are more sensitive to these photons). In view of our interest in understanding the BATSE observations, we concentrate on the behavior of the electrons with  $\gamma_e \approx \hat{\gamma}_e$ . We do retain a scaling factor in terms of the observed photon energy  $h\nu_{\text{obs}}$  in the results so that the cooling times of other electrons are also implicit in our relations.

Using equation (18), we calculate  $\hat{\gamma}_e$  to be given by

$$\hat{\gamma}_e = \left( \frac{m_e c h \nu_{\text{obs}}}{\hbar q_e \gamma_2 B} \right)^{1/2} = 1.7 \times 10^4 \epsilon_B^{-1/4} \left( \frac{h \nu_{\text{obs}}}{100 \text{ keV}} \right)^{1/2} \times \left( \frac{t_{\text{dur}}}{10 \text{ s}} \right)^{3/8} l_{18}^{-3/8} n_1^{-1/4}. \quad (21)$$

First we need to check that electrons with  $\gamma_e = \hat{\gamma}_e$  are available in the shocked material. This means that we require  $\gamma_{e,\text{min}} < \hat{\gamma}_e$ , which corresponds to the condition

$$\epsilon_{e|r} < 28 \epsilon_B^{-1/4} \left( \frac{h \nu_{\text{obs}}}{100 \text{ keV}} \right)^{1/2} \left( \frac{t_{\text{dur}}}{10 \text{ s}} \right)^{3/8} \zeta^{3/4} l_{18}^{-3/8} n_1^{-1/4}, \quad (22)$$

in the reverse shock, and the condition

$$\epsilon_{e|f} < 0.1 \epsilon_B^{-1/4} \left( \frac{h \nu_{\text{obs}}}{100 \text{ keV}} \right)^{1/2} \left( \frac{t_{\text{dur}}}{10 \text{ s}} \right)^{3/4} l_{18}^{-3/4} n_1^{-1/4}, \quad (23)$$

in the forward shock. Since by definition  $\epsilon_e \leq 1$ , we see that the reverse shock always has electrons with the right Lorentz factors to produce synchrotron photons within the BATSE range. However, the situation is more doubtful in the case of the forward shock. If the heating of the electrons is efficient, i.e., if  $\epsilon_{e|f} \sim 1$ , and if the burst has a short duration, then most of the electrons may be too energetic to produce BATSE-visible photons. Of course, as an electron cools, it radiates at progressively softer energies. Therefore, even if  $\gamma_{\text{min}}$  is initially too large for the synchrotron radiation to be visible to BATSE, the same electrons would be at a later time have  $\gamma_e \sim \hat{\gamma}_e$  and become visible to BATSE. However, the energy remaining in the electrons at the later time will also be lower (by a factor  $\hat{\gamma}/\gamma_{\text{min}}$ ), which means that the burst will be inefficient. For simplicity, we ignore this radiation.

Substituting the value of  $\hat{\gamma}_e$  from equation (21) into the cooling rate equation (20), we obtain the cooling timescale as a function of the observed photon energy to be

$$\tau_{\text{syn}} = (1.4 \times 10^{-2} \text{ s}) \epsilon_B^{-3/4} \left( \frac{h \nu_{\text{obs}}}{100 \text{ keV}} \right)^{-1/2} \times \left( \frac{t_{\text{dur}}}{10 \text{ s}} \right)^{3/4} l_{18}^{-3/4} n_1^{-3/4}. \quad (24)$$

Equation (24) is valid for both the forward and reverse shock and is moreover independent of whether the reverse shock is relativistic or Newtonian. It is therefore quite a robust result.

The cooling time calculated above sets a lower limit to the variability timescale of a GRB, since the burst cannot possibly contain spikes that are shorter than its cooling time. Observations of GRBs typically show asymmetric spikes in the intensity variation, where a peak generally has a fast rise and a slower exponential decline (FRED). A

plausible explanation of this observation is that the shock heating of the electrons happens rapidly (though episodically), and that the rise time of a spike is related to the heating time. The decay time is then set by the cooling, so that the widths of spikes directly measure the cooling time.

We see from equation (24) that  $\tau_{\text{syn}}$  is proportional to  $(h\nu)^{-1/2}$ . This suggests that there should be an inverse correlation between the width of a spike and the energy band in which the observation is made. An inverse correlation has indeed been observed (Fenimore et al. 1995). In fact, even the predicted dependence as the inverse square root of the photon energy is quite close to the observed index of  $-0.4$ .

Using equations (24) and (3), we can estimate the duty cycle  $D$  of the variability as the ratio of the cooling timescale to the total duration:

$$D \equiv \frac{\tau_{\text{syn}}}{t_{\text{dur}}} = 1.4 \times 10^{-3} \epsilon_B^{-3/4} \left( \frac{h \nu_{\text{obs}}}{100 \text{ keV}} \right)^{-1/2} \times \left( \frac{t_{\text{dur}}}{10 \text{ s}} \right)^{-1/4} l_{18}^{-3/4} n_1^{-3/4}. \quad (25)$$

We see that the duty cycle depends only weakly on the burst duration. Observationally, it appears to be true that the narrowest features in a burst are a constant fraction of the total duration, independent of the actual duration of a burst (e.g., Bhat et al. 1994), but this prediction of the model needs to be checked in more detail against observations.

Most GRBs are seen to be highly variable with duty cycles significantly smaller than unity, typically on the order of 5% or less. Using this as a constraint, we obtain a lower limit to the value of  $\epsilon_B$ :

$$\epsilon_B \geq 8.4 \times 10^{-3} \left( \frac{D}{0.05} \right)^{-4/3} \left( \frac{h \nu_{\text{obs}}}{100 \text{ keV}} \right)^{-2/3} \times \left( \frac{t_{\text{dur}}}{10 \text{ s}} \right)^{-1/3} l_{18}^{-1} n_1^{-1}. \quad (26)$$

This suggests that the magnetic field energy density cannot be far less than the equipartition value in the radiation-emitting regions in GRBs. Clearly, the limit is valid only if synchrotron radiation is the main cooling process. In particular, we have ignored so far the inverse Compton process, which could increase the emission and thereby allow a lower value of  $\epsilon_B$ . We turn now to the implications of inverse Compton scattering.

#### 4. INVERSE COMPTON SCATTERING

Inverse Compton (IC) scattering may modify our analysis in three ways.

First, a significant fraction of the synchrotron emission may be scattered so that the observed synchrotron flux is lower than the calculated value. In fact, this is never the case because we can show that the emitting regions are always extremely optically thin.

Second, IC might scatter low-energy synchrotron photons into the BATSE energy band, so that some of the observed radiation may be due to IC rather than synchrotron emission. We show that this is again not the case. IC photons from the forward shock are always much harder than the BATSE range. Although IC photons from the reverse shock can fall within the BATSE range, they do so

only for bursts with large duty cycles, i.e., for smooth one-hump bursts that form only a minority of the observed bursts.

Finally, even if IC does not influence any of the observed photons, it may speed up the cooling of the emitting regions and therefore shorten the cooling time that we estimated earlier under the assumption of pure synchrotron emission. This effect is unimportant for the forward shock but could be important for the reverse shock under certain conditions.

Let us begin with the optical depth. The radial thicknesses of zones 2 and 3 are each of order  $\gamma_2 \Delta$  in the co-moving frame. Therefore, the Thomson optical depth across the full radial extent of both zones is given by

$$\tau = (n_3 \gamma_2 \Delta + n_2 \gamma_2 \Delta) \sigma_T = 4 \times 10^{-6} \left( \frac{t_{\text{dur}}}{10 \text{ s}} \right)^{-1/8} \xi^{-3/4} n_1, \quad (27)$$

where we have used the inequality  $n_2 \ll n_3$ . In fact, this is an overestimate of  $\tau$ , since some electrons are very energetic and have a reduced scattering cross section by the Klein-Nishina effect. Even without allowing for this effect, we see that the optical depth is extremely small for reasonable parameters.

Considering the second point, synchrotron photons emitted by electrons of Lorentz factor  $\gamma_{e,1}$  and inverse Compton scattered by electrons of  $\gamma_{e,2}$  have an observed energy of

$$\begin{aligned} (h\nu_{\text{IC}})_{\text{obs}} &= \frac{\hbar q_e B}{m_e c} \gamma_{e,1}^2 \gamma_{e,2}^2 \gamma_2 \\ &= 350 \text{ MeV} \left( \frac{\gamma_{e,1}}{10^3} \right)^2 \left( \frac{\gamma_{e,2}}{10^3} \right)^2 \\ &\quad \times \epsilon_B^{1/2} \left( \frac{t_{\text{dur}}}{10 \text{ s}} \right)^{-3/4} l_{18}^{3/4} n_1^{1/2}. \end{aligned} \quad (28)$$

For a photon to be detectable in BATSE, its observed energy has to be in the range 25 keV to about 1 MeV. This requires  $\gamma_{e,1} \gamma_{e,2} < 200$ . Now, if we consider an efficient burst with  $\epsilon_e \sim 1$ , then the typical value of  $\gamma_{e,\text{min}}$  is  $\gg 1000$  for the forward shock and is  $> 1000$  even for the reverse shock if it is relativistic. Only for a Newtonian reverse shock (where  $\xi \sim 1$ ) with somewhat low efficiency ( $\epsilon_e < 0.3$ ) is  $\gamma_{e,\text{min}} < 1000$ . Stating this differently, the condition  $\gamma_{e,\text{min}} < 200$  yields, using equation (11), an extremely small  $\epsilon_e$  for the forward shock:

$$\begin{aligned} \epsilon_e &< 7.6 \times 10^{-4} \epsilon_B^{-1/8} \left( \frac{h\nu_{\text{obs}}}{100 \text{ keV}} \right)^{1/4} \\ &\quad \times \left( \frac{t_{\text{dur}}}{10 \text{ s}} \right)^{9/16} l_{18}^{-9/16} n_1^{-1/8}, \end{aligned} \quad (29)$$

while for the reverse shock we obtain

$$\epsilon_e < 0.21 \epsilon_B^{-1/8} \left( \frac{h\nu_{\text{obs}}}{100 \text{ keV}} \right)^{1/4} \left( \frac{t_{\text{dur}}}{10 \text{ s}} \right)^{3/16} \xi^{3/4} l_{18}^{-3/16} n_1^{-1/8}. \quad (30)$$

IC photons from the forward shock are thus completely out of the range of BATSE unless  $\epsilon_e$  is extremely small, a possi-

bility that we eliminate on the grounds of inefficiency (see the discussion in the Introduction). With the reverse shock, the best chance is with  $\xi$  equal to its largest value, namely,  $\xi = 1$ , and considering a long burst duration. We show below that even this case results in a long cooling time and a large duty cycle, and therefore it is ruled out by the observed peaky nature of bursts.

We turn next to the question of whether IC losses can alter significantly the cooling timescale of the electrons with Lorentz factor  $\hat{\gamma}_e$  that emit the synchrotron radiation observed by BATSE. Because of the Klein-Nishina effect, the cross section for Compton scattering decreases quite rapidly when the energy of the synchrotron photons becomes larger than  $m_e c^2$  in the electron rest frame. IC is therefore most important when the synchrotron photons are below this Klein-Nishina cutoff. We simplify matters by assuming that IC switches off completely once the Klein-Nishina regime is entered. This is, of course, a rather severe simplification, but we consider it justified for the purposes of the present argument. The lowest energy synchrotron photons available are those photons emitted by the lowest energy electrons, with  $\gamma_{e1} = \gamma_{e,\text{min}}$  (eq. [11]). The IC process can be neglected if even these low-energy photons are in the Klein-Nishina range for an electron of Lorentz factor  $\hat{\gamma}_e$ , i.e., if

$$(h\nu_{\text{min}})_{\text{fluid}} \hat{\gamma}_e \geq m_e c^2. \quad (31)$$

Using the formula for  $(h\nu)_{\text{fluid}}$  given in equation (17) and setting  $\gamma_e = \gamma_{e,\text{min}}$  (eqs. [15] or [16]) and substituting the values of  $e$  and  $n$  (eqs. [4] or [5]), we find that IC can be neglected if

$$\epsilon_e > 2.9 \times 10^{-2} \epsilon_B^{-1/8} \left( \frac{h\nu_{\text{obs}}}{100 \text{ keV}} \right)^{-1/4} \left( \frac{t_{\text{dur}}}{10 \text{ s}} \right)^{3/8} l_{18}^{-3/8} n_1^{-1/8}, \quad (32)$$

for the forward shock, and if

$$\epsilon_e > 8.0 \epsilon_B^{-1/8} \left( \frac{h\nu_{\text{obs}}}{100 \text{ keV}} \right)^{-1/4} \xi^{3/4} n_1^{-1/8}, \quad (33)$$

for the reverse shock.

Since on the grounds of efficiency we have argued that  $\epsilon_e$  must be close to unity, we see that the condition in the case of the forward shock is almost always satisfied, and therefore IC cooling is never important there. The reverse shock, on the other hand, never satisfies the condition, and so IC cooling might be important.

Since IC is unimportant for the forward shock, the relations (25) and (26) derived in § 3 are valid without any change. However, for the reverse shock, we need to calculate the true cooling time including the additional cooling due to IC. To do this, we use the following model. The energy density available for conversion to radiation is the electron energy density,  $U_e$ . Eventually all this energy is radiated by synchrotron or by IC. We denote the former by  $U_{\text{syn}}$  and the latter by  $U_{\text{IC}}$ :

$$U_e = U_{\text{syn}} + U_{\text{IC}}. \quad (34)$$

If the shock has already propagated for a period of time longer than the cooling time, we expect a steady state radiation density profile to be present in the vicinity of the shock-heated electrons. In this steady state, we expect the energy flux given by the shock to the electrons to be equal

to the radiation flux. Further, since the shock front moves with a velocity equal to a fraction of the speed of light, the total radiation density must be comparable to  $U_e$ , with the synchrotron and IC densities given respectively by  $U_{\text{syn}}$  and  $U_{\text{IC}}$ .

Because of the Klein-Nishina effect, we need consider only one scattering of each photon, and further scatterings are highly suppressed. In this limit, the Compton  $y$  parameter is directly equal to the ratio of the rate of IC energy loss to the rate of synchrotron energy loss. At the same time,  $y$  is also equal to the ratio of the energy density in soft radiation (in our case synchrotron) to magnetic field energy density (Rybicki & Lightman 1979). Therefore, we find

$$y = \frac{U_{\text{IC}}}{U_{\text{syn}}} = \frac{U_{\text{syn}}}{U_B}. \quad (35)$$

Recalling that  $U_e = \epsilon_e e$  and  $U_B = \epsilon_B e$ , we can solve equations (34) and (35) to obtain

$$y \equiv \frac{U_{\text{IC}}}{U_{\text{syn}}} = \frac{\epsilon_e}{\epsilon_B} \quad \text{if } \frac{\epsilon_e}{\epsilon_B} \ll 1, \quad (36)$$

$$y \equiv \frac{U_{\text{IC}}}{U_{\text{syn}}} = \sqrt{\frac{\epsilon_e}{\epsilon_B}} \quad \text{if } \frac{\epsilon_e}{\epsilon_B} \gg 1. \quad (37)$$

If  $\epsilon_e < \epsilon_B$ , we see that  $y < 1$  and IC cooling is not important. In this case, we can use equations (25) and (26) even for the reverse shock. However, if  $\epsilon_e > \epsilon_B$ , then  $\gamma \sim (\epsilon_e/\epsilon_B)^{1/2} > 1$  and most of the emitted radiation comes out as IC photons. The cooling rate of the relevant electrons then increases by the factor of  $y$ , and the lower limit to the magnetic energy density set by the observed duty cycle decreases. Equations (25) and (26) are thus replaced by

$$D = \frac{\tau_{\text{syn}}}{t_{\text{dur}}} = 1.4 \times 10^{-3} \epsilon_e^{-1/2} \epsilon_B^{-1/4} \left( \frac{h\nu_{\text{obs}}}{100 \text{ keV}} \right)^{-1/2} \times \left( \frac{t_{\text{dur}}}{10 \text{ s}} \right)^{-1/4} l_{18}^{-3/4} n_1^{-3/4}. \quad (38)$$

$$\epsilon_B \geq 6 \times 10^{-7} \epsilon_e^{-2} \left( \frac{D}{0.05} \right)^{-4} \left( \frac{h\nu_{\text{obs}}}{100 \text{ keV}} \right)^{-2} \left( \frac{t_{\text{dur}}}{10 \text{ s}} \right)^{-1} l_{18}^{-3} n_1^{-3}. \quad (39)$$

We emphasize that these estimates are relevant only for the reverse shock and only if  $\epsilon_e > \epsilon_B$ . For all other cases, we use equations (25) and (26).

Although the duty cycle argument now appears to allow a much lower magnetic energy density,  $\epsilon_B$  as low as  $10^{-6}$ , we obtain another more stringent limit by demanding that the burst be efficient. Since the IC photons are too hard to be observed by BATSE, the observed efficiency decreases by a factor  $1/y = (\epsilon_B/\epsilon_e)^{1/2}$ . Thus, even if we take the maximum efficiency for the shock acceleration of electrons,  $\epsilon_e = 0.5$ , still we find that a value of  $\epsilon_B \sim 10^{-6}$  results in a burst with an efficiency  $< 10^{-3}$  just from this effect. In fact, the efficiency is a little lower for reasons described in the next section. As we explained in the Introduction, GRB scenarios become quite implausible at such low efficiencies, as they would imply unreasonably large energies in the original explosion.

We are now ready to show, as we have stated at the beginning of this section, that we cannot have a highly vari-

able burst of IC photons from the reverse shock. The Lorentz factor of electrons emitting IC photons with energy  $h\nu$  is given by equation (28) as

$$\gamma_e = \left( \frac{m_e c h \nu}{\hbar q_e \gamma_2 B} \right)^{1/4}. \quad (40)$$

The corresponding duty cycle for these electrons is

$$\frac{\tau_{\text{syn}}}{t_{\text{dur}}} = 0.18 \left( \frac{t_{\text{dur}}}{10 \text{ s}} \right)^{-1/16} \epsilon_B^{-3/8} \epsilon_e^{-1/2} \times \left( \frac{h\nu}{100 \text{ keV}} \right)^{-1/4} l_{18}^{-15/16} n_1^{-7/8}. \quad (41)$$

As we have already seen, electrons with a Lorentz factor given by equation (40) are impossible in the forward shock but are possible in a Newtonian reverse shock provided  $\epsilon_e < 0.2$ . However, now we see from the above equation that even if these electrons are present, their radiation will come out with a somewhat large duty cycle  $\sim 1$ . This is ruled out by the observations.

We note that Mészáros et al. (1993) choose as the canonical values for their models  $\epsilon_B = 10^{-5}$  and  $\epsilon_e \approx 1$ . The duty cycle for this choice of parameters is  $\sim 10$ , which means that the hydrodynamic time is an order of magnitude shorter than the cooling time. This runs into problems on two counts. First the model can only produce smooth single-hump bursts and cannot explain the variability of observed bursts without invoking substructure within the shell. Second, the hydrodynamical conditions in the expanding shell, in particular  $\gamma_2$ , change on the hydrodynamic time-scale. This means that only during the first  $t_{\text{hyd}}$  of cooling will the radiation be fully beamed with the Lorentz factor  $\gamma_2$ . The later cooling will be less beamed and will therefore be smeared out significantly in observer time. What this means is that for the observer, the burst will effectively last only for a duration  $t_{\text{hyd}}$ ; the remaining 90% of the energy will come much later, will be weaker and softer, and will not be counted as part of the burst. As a result, the observed efficiency of the burst will be reduced by a factor of order 10.

## 5. EFFICIENCY

We consider now the efficiencies with which the two shocks convert their thermal energy into observable radiation. Two important factors influence the efficiency and lower it from the ideal value of unity. First, only the electrons cool, which means that only a fraction  $\epsilon_e$  of the total thermal energy is available to be radiated. Second, a significant fraction of the radiated energy may lie outside the BATSE energy range because (1) the synchrotron emission is usually spread over a large energy range, and (2) much of the cooling may happen via IC scattering whose radiation is quite generally at energies above the BATSE range.

We have assumed a power-law distribution of electron energy with a power-law index  $\beta = -2.5$ . This index has been chosen such that the time-integrated synchrotron emission corresponds to a power-law radiative spectrum with index  $\beta = -2.25$ , in agreement with the observations (Band et al. 1993). The fraction of the synchrotron power that is radiated in the BATSE band (at around 100 keV) is then given by

$$\epsilon_{\text{syn}} = \left( \frac{h\nu_{\text{min}}}{100 \text{ keV}} \right)^{-\beta-2} = \left( \frac{h\nu_{\text{min}}}{100 \text{ keV}} \right)^{0.25}, \quad (42)$$

where  $h\nu_{\min}$  is the observed photon energy corresponding to the synchrotron radiation from electrons with  $\gamma_e = \gamma_{e,\min}$ .

For the forward shock, we can calculate  $h\nu_{\min}$  using equation (18) and setting  $\gamma_e = \gamma_{e,\min}$  from equation (15):

$$\frac{h\nu_{\min}}{100 \text{ keV}} = 100\epsilon_e^2 \epsilon_B^{1/2} \left( \frac{t_{\text{dur}}}{10 \text{ s}} \right)^{-3/2} l_{18}^{3/2} n_1^{1/2}. \quad (43)$$

Since IC scattering is unimportant for the forward shock, the net efficiency is just the product of  $\epsilon_e$ , the fraction of the energy that goes into the electrons, and the synchrotron efficiency factor  $\epsilon_{\text{syn}}$  given above. Thus, we find the total efficiency of the forward shock to be

$$\epsilon_{\text{tot},f} = \epsilon_e \epsilon_{\text{syn}} = 3.2\epsilon_e^{3/2} \epsilon_B^{1/8} \left( \frac{t_{\text{dur}}}{10 \text{ s}} \right)^{-3/8} l_{18}^{3/8} n_1^{1/8} \quad (44)$$

The efficiency is of order unity whenever the forward shock is visible in the BATSE range (which requires long durations as discussed in § 3).

For the reverse shock, we have

$$\frac{h\nu_{\min}}{100 \text{ keV}} = 1.3 \times 10^{-3} \epsilon_e^2 \epsilon_B^{1/2} \left( \frac{t_{\text{dur}}}{10 \text{ s}} \right)^{-3/4} \xi^{-3/2} l_{18}^{3/4} n_1^{1/2} \quad (45)$$

In the case of the reverse shock, IC scattering has the possibility of affecting the cooling time and thereby the efficiency. If  $\epsilon_e < \epsilon_B$ , we have seen that the  $y$  parameter is less than unity and the overall efficiency is just given by

$$\epsilon_{\text{tot},r} = \epsilon_e \epsilon_{\text{syn}} = 0.19\epsilon_e^{3/2} \epsilon_B^{1/8} \left( \frac{t_{\text{dur}}}{10 \text{ s}} \right)^{-3/16} \times \xi^{-3/8} l_{18}^{3/16} n_1^{1/8}, \quad \epsilon_e < \epsilon_B. \quad (46)$$

However, if  $\epsilon_e > \epsilon_B$ , then  $y = (\epsilon_e/\epsilon_B)^{1/2} > 1$  and the efficiency is reduced further to

$$\epsilon_{\text{tot},r} = \frac{\epsilon_e \epsilon_{\text{syn}}}{y} = 0.19\epsilon_e \epsilon_B^{5/8} \left( \frac{t_{\text{dur}}}{10 \text{ s}} \right)^{-3/16} \times \xi^{-3/8} l_{18}^{3/16} n_1^{1/8}, \quad \epsilon_e > \epsilon_B.$$

We can see from these expressions that efficient bursts are possible only if  $\epsilon_e$  is high. The value of  $\epsilon_B$  is important, as far as efficiency is concerned, only if  $\epsilon_e > \epsilon_B$ , and that too only for the reverse shock. We give some specific estimates of the efficiency in different regions of the parameter space in the following sections.

## 6. EXPLORATION OF THE PARAMETER SPACE

We have introduced several parameters in the previous sections. Two of these are relatively well known, namely, the ISM density  $n_1 \sim 1 \text{ cm}^{-3}$  and the explosion energy  $E$ , which determines the Sedov length scale  $l \sim 10^{18} \text{ cm}$ . Four other parameters are essentially unknown.

Two “external parameters” depend on the properties of the initial fireball and are likely to vary from one explosion to the next:

1. The Lorentz factor of the shell  $\gamma$ .
2. The shell thickness  $\Delta$ , which we prefer to replace by the parameter  $\xi$  defined in equation (2). As already explained,  $\xi < 1$  for a relativistic reverse shock and  $\xi = 1$  for a spreading Newtonian shell.

The above two parameters determine the Lorentz factor  $\gamma_2 = \gamma \xi^{3/4}$  of the shocked material and the hydrodynamic time (eq. [3]) on which the kinetic energy of the expanding

shell is converted to thermal energy. In the case of the forward shock,  $\gamma_2$  also determines the thermal energy density and the particle density of the postshock gas. Therefore, all observables from the forward shock are functions only of  $\gamma_2$  rather than of  $\gamma$  and  $\xi$  individually. We prefer to express our results in terms of the observed burst duration  $t_{\text{dur}}$  rather than  $\gamma_2$ , using equation (6) to convert from one to the other. The reverse shock is more complicated, as the results depend in general on both  $\gamma$  and  $\xi$ . We choose to express our results as functions of  $t_{\text{dur}}$  and  $\xi$ , using equations (2) and (3) to transform from  $\gamma, \xi$ .

In addition to the above two “external parameters,” there are two “internal parameters” that depend on the unknown details of the microphysics in the shocked regions:

3. The energy density in the magnetic field that we describe by means of the field equipartition parameter,  $\epsilon_B$ .
4. The fraction of the thermal energy that goes into the electrons,  $\epsilon_e$ .

Our current understanding of field amplification and particle acceleration in ultrarelativistic shocks is quite primitive, and it is not possible to estimate either of these parameters from first principles. Therefore, we treat them as free parameters and try to deduce their values from the constraints imposed by the GRB observations. We do, however, assume that the parameters are relatively constant from one burst to another and between the forward and reverse shock. This assumption may well be wrong, but we make it in the interests of simplicity.

Overall, we have a three-dimensional parameter space,  $t_{\text{dur}} \epsilon_B \epsilon_e$ , for the forward shock, and a four-dimensional parameter space  $t_{\text{dur}} \xi \epsilon_B \epsilon_e$ , for the reverse shock. Figures 2 and 3 summarize all the ideas of the previous sections for the forward shock and reverse shock, respectively.

Figure 2 shows the  $\epsilon_B \epsilon_e$  plane for the forward shock for four choices of the observed burst duration  $t_{\text{dur}}$ . The forward shock tends to be very energetic so that even the electrons with the lowest Lorentz factor  $\gamma_{e,\min}$  often radiate their synchrotron emission above the BATSE energy range. Such cases are not of interest here because they do not contribute to the BATSE database. Taking a nominal cutoff energy of 400 keV to represent the BATSE threshold (for example, more than half the 54 bursts analyzed by Band et al. have their break energy between 100 keV and 400 keV), we show by the shaded regions in Figure 2 the parameter space that is inaccessible to BATSE. If BATSE is to detect radiation from the forward shock, the parameters must correspond to the unshaded regions. In general, we see that the forward shock is more likely to be visible to BATSE in a long burst than in a short burst.

The panels in Figure 2 show two sets of contours: the solid lines indicate contours of constant duty cycle, calculated with equation (25), while the dashed lines indicate contours of constant efficiency, calculated with equation (44). Recall that the forward shock cools almost exclusively by synchrotron emission and has very little IC scattering. For a given  $t_{\text{dur}}$ , the duty cycle depends only on  $\epsilon_B$  and is independent of  $\epsilon_e$ . If we use the typical observed duty cycle of a few percent as a constraint, we see that the forward shock needs  $\epsilon_B \sim 10^{-2}$ . The efficiency of the forward shock is primarily a function of  $\epsilon_e$ , with some weak dependence on  $\epsilon_B$  from the fact that a small fraction of the emitted radiation may be below the BATSE range (eq. [42]). This is

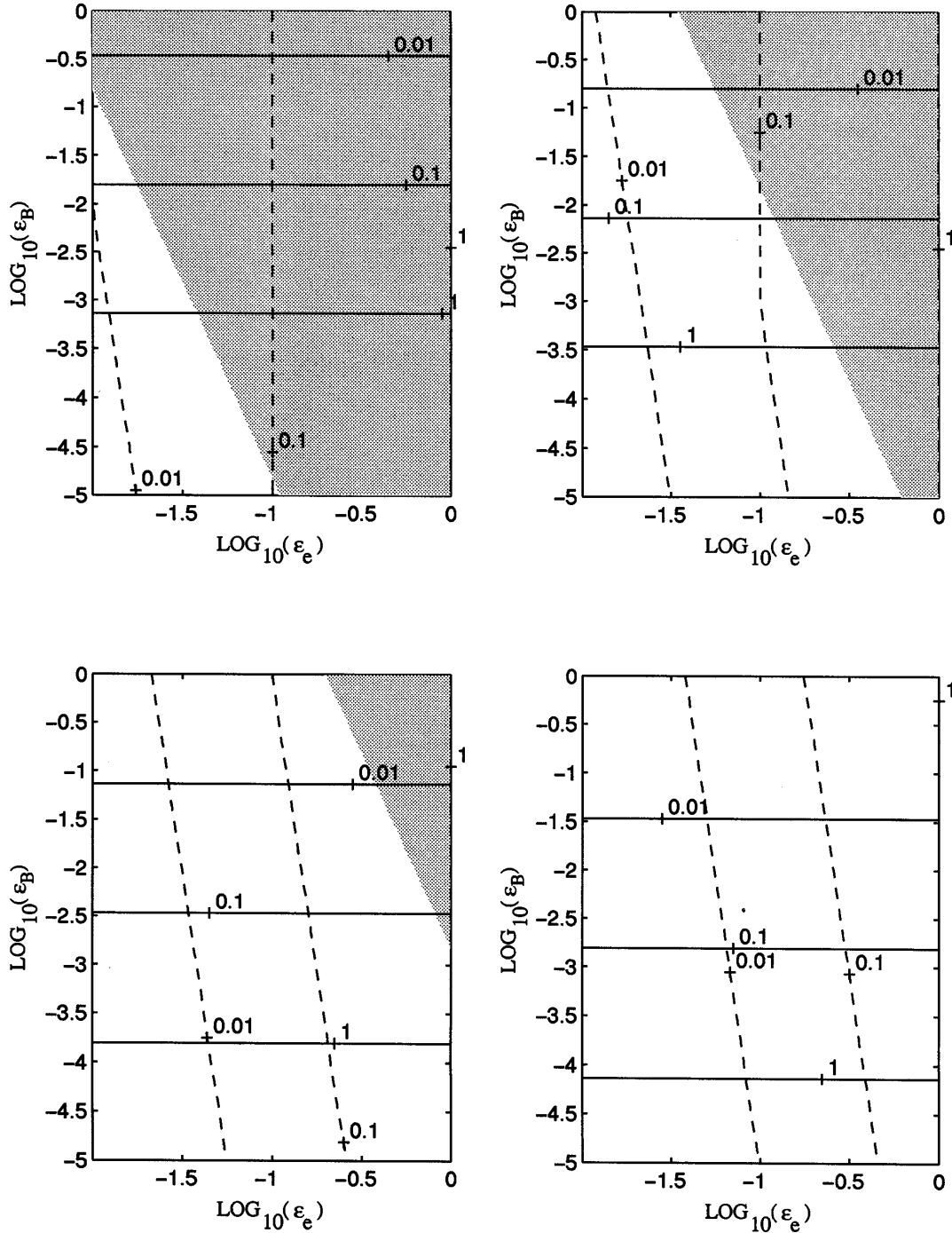


FIG. 2.—Properties of the forward shock for four burst durations. *Top left*:  $t_{\text{dur}} = 0.1$  s; *top right*: 1 s; *bottom left*: 10 s; *bottom right*: 100 s. Solid lines show contours of the duty cycle, and dashed lines show contours of burst efficiency, as functions of the two parameters,  $\epsilon_B$  and  $\epsilon_e$ . In the shaded regions, even the lowest energy electrons in the postshock medium produce most of their synchrotron radiation above 400 keV in the observer frame. Such bursts are not visible to BATSE.

usually a small factor, since the electrons in the forward shock are usually very energetic. If we wish to have reasonable efficiencies, then the forward shock requires  $\epsilon_e$  close to unity (certainly larger than about 0.1).

For the choice  $\epsilon_B \sim 10^{-2}$ ,  $\epsilon_e \sim 1$ , Figure 2 shows that the forward shock radiation is visible to BATSE only for somewhat long bursts with  $t_{\text{dur}}$  greater than about 10 s. If we increase  $\epsilon_B$  also to be of order unity, then only very long bursts of 100 s duration or longer would be visible to BATSE.

Figure 3 shows the results corresponding to the reverse shock. In this case, we need to specify both external parameters,  $t_{\text{dur}}$  and  $\xi$ , to describe the shock, and therefore we display six panels covering three values of  $t_{\text{dur}}$  and two values of  $\xi$ . Note that  $\xi = 1$  corresponds to a Newtonian reverse shock and  $\xi < 1$  corresponds to a relativistic shock.

The reverse shock is always less energetic than the forward shock, and its synchrotron photons are almost always soft enough to be within the BATSE range. The gray “undetected” regions are therefore limited to an extreme

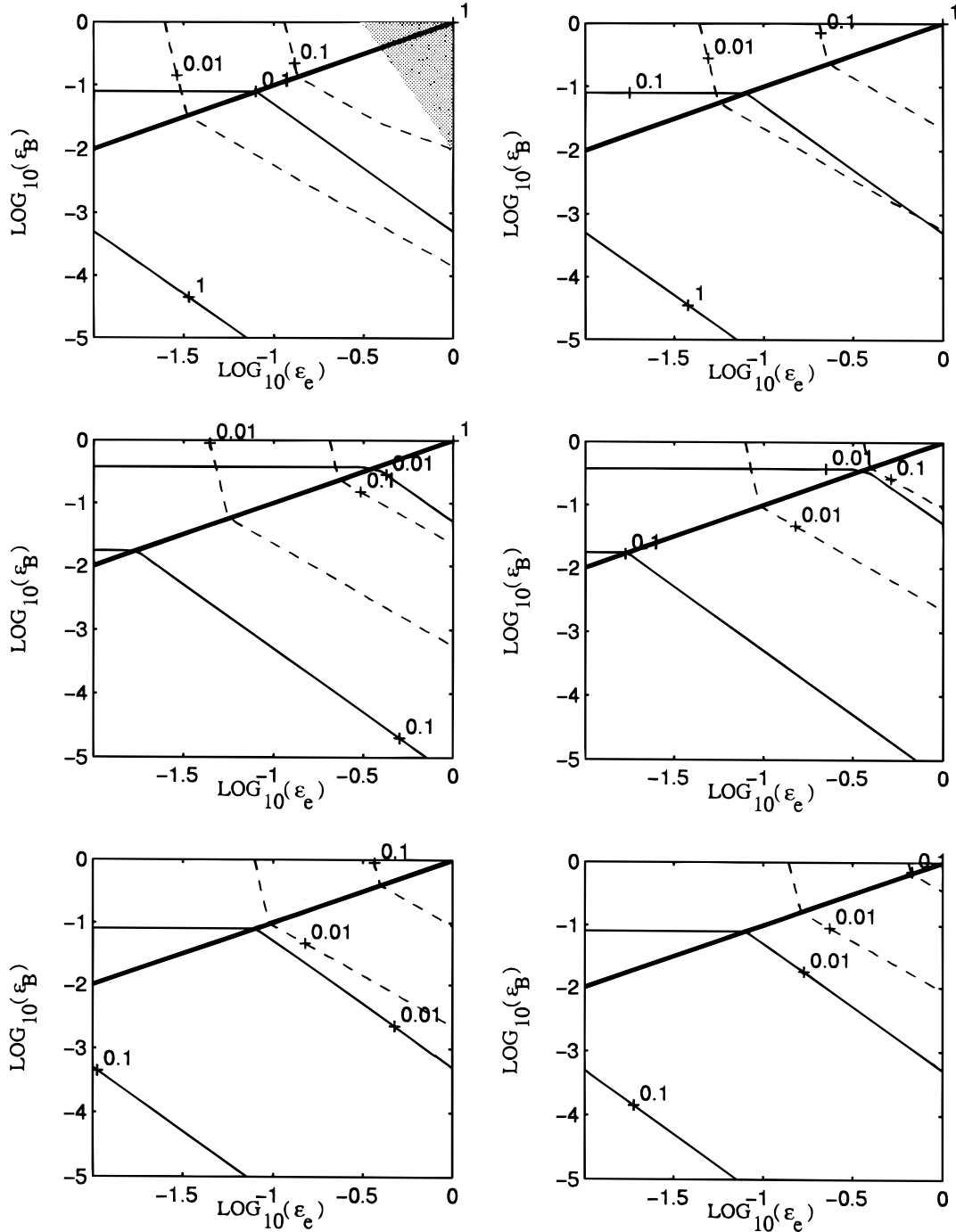


FIG. 3.—Similar to Fig. 2, but for the reverse shock. The six panels are as follows. *Top left*:  $t_{\text{dur}} = 0.001$  s,  $\xi = 0.1$  ( $\gamma = 5 \times 10^4$ ); *top right*:  $t_{\text{dur}} = 0.001$  s,  $\xi = 1$  ( $\gamma = 8000$ ); *middle left*:  $t_{\text{dur}} = 0.1$  s,  $\xi = 1$  ( $\gamma = 8000$ ); *middle right*:  $t_{\text{dur}} = 0.1$  s,  $\xi = 1$  ( $\gamma = 1600$ ); *bottom left*:  $t_{\text{dur}} = 10$  s,  $\xi = 0.1$  ( $\gamma = 1600$ ); *bottom right*:  $t_{\text{dur}} = 10$  s,  $\xi = 1$  ( $\gamma = 280$ ); All unshaded regions are visible to BATSE. The thick lines correspond to  $\epsilon_B = \epsilon_e$ . IC scattering enhances the cooling below this line, leading to loss of efficiency of bursts.

corner of the parameter space. In addition, the soft nature of the synchrotron radiation means that the Klein-Nishina effect is not important for IC scattering. Whether or not IC is important is therefore determined solely by the relative magnitude of  $\epsilon_B$  and  $\epsilon_e$ . IC is important if  $\epsilon_B < \epsilon_e$ , and it is not in the opposite case. The boundary between the two regimes is indicated by the thick lines in Figure 3, with IC being important below the line.

Above the thick lines, the dependences of duty cycle and efficiency on  $\epsilon_B$  and  $\epsilon_e$  are similar to those shown for the forward shock (Fig. 2). The only difference is that the effi-

ciency of the reverse shock is generally lower than that of the forward shock because the bulk of the synchrotron emission occurs below the BATSE range. In the regions below the thick lines in Figure 3, where IC is important, the duty cycle is modified relative to the pure synchrotron case. Because of this, the solid lines are tilted and take on a dependence on  $\epsilon_e$ . The efficiency also is influenced by IC scattering, since it scatters a considerable part of the energy above the BATSE range.

As  $\gamma$  decreases, the reverse shock becomes cooler, and it emits less and less photons into the BATSE range. The

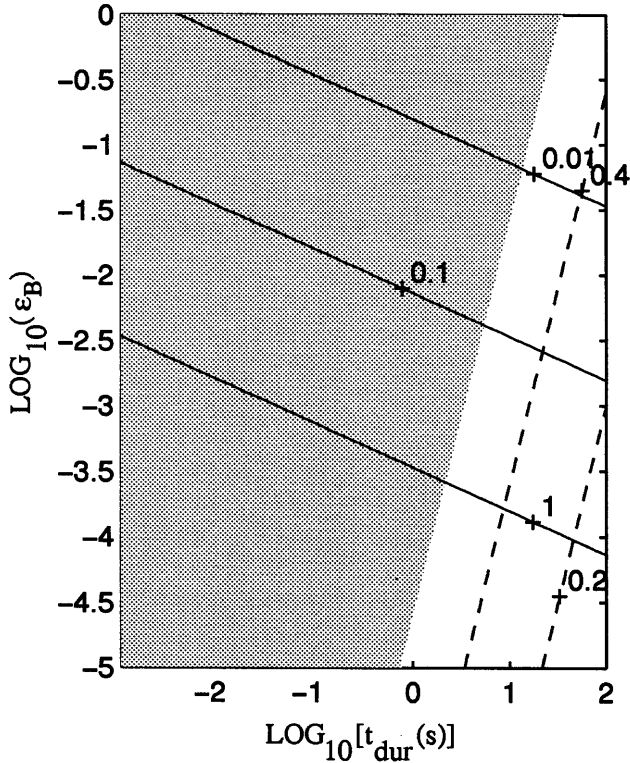


FIG. 4.—Contours of duty cycle (solid lines) and efficiency (dashed lines) for the forward shock as a function of  $\epsilon_B$  and  $t_{\text{dur}}$ . The results correspond to the choice  $\epsilon_e = 0.5$ . BATSE can observe bursts only in the unshaded region of the diagram.

reverse shock is, therefore, efficient only for short durations ( $< 0.1$  s). As with the forward shock, the value of  $\epsilon_B$  must be relatively high in order to obtain bursts with short duty cycles. The demand here is, however, a little weaker in the IC zone (below the thick lines). Similarly, high values of  $\epsilon_e$  are needed in order to obtain high efficiency. Indeed, for long duration bursts, even with  $\epsilon_e \sim 1$  the efficiency is only about 10%.

Although Figures 2 and 3 include almost all the information we need, it is instructive to look at simpler plots corresponding to more restricted conditions. Specifically, we set  $\epsilon_e = 0.5$ , corresponding to half the thermal energy of the shocks going into the electrons. This is the largest plausible value for this parameter. We feel that it is necessary to select such a high value because burst efficiency is quite a strong constraint and in many source models the observed GRB energies (within the cosmological scenario) are barely possible even with  $\epsilon_e \sim 1$ .

In Figure 4, we show the results for the forward shock in the  $t_{\text{dur}}\epsilon_B$  plane, while in Figure 5 we show four panels of  $t_{\text{dur}}\epsilon_B$  for the reverse shock.

In general, we see that for a given choice of  $t_{\text{dur}}$  and  $\epsilon_B$ , only one of the two shocks is important. For long durations (which correspond to relatively low values of  $\gamma$ ), the reverse shock is too soft and is inefficient in the BATSE band, and so the BATSE signal is dominated by the efficient forward shock. On the other hand, for short durations (where  $\gamma$  is relatively high), the reverse shock is more efficient, while the forward shock is too hard and radiates outside the BATSE range. This systematic difference between the two shocks leads to a possible scenario to explain the observed bimodal distribution of burst durations. The scenario is described in the next section.

Figures 4 and 5 also confirm once again that we need a fairly large  $\epsilon_B$  ( $> 10^{-2}$ ). This requirement comes from two directions. First,  $\epsilon_B > 10^{-2}$  is necessary in order to have a duty cycle in the forward shock of a few percent. Second, it is needed if we do not wish to reduce the efficiency of the reverse shock too much. Although we could in principle choose a value of  $\epsilon_B$  anywhere between  $10^{-2}$  and 1, we prefer to set  $\epsilon_B \sim 10^{-2}$  because for this choice the forward shock is visible to BATSE down to durations  $\sim 10$  s, whereas with  $\epsilon_B \sim 1$  the forward shock is detectable only for  $t_{\text{dur}} > 30$  s.

## 7. BIMODALITY OF BURST DURATIONS

As an example of the implications of the analysis presented in this paper, we describe here a scenario that provides a possible explanation for the observed bimodality of GRB durations.

We assume that all bursts have the same values of  $n_1$ ,  $l_{18}$ ,  $\xi$ ,  $\epsilon_B$ , and  $\epsilon_e$  and that the only parameter that distinguishes one burst from another is the Lorentz factor  $\gamma$  of the expansion of the relativistic shell. This is obviously much too simple. Nevertheless, even this simple model provides a nice separation of observed bursts into two classes: short bursts in which BATSE detects radiation only from the reverse shock, and long bursts in which most of the BATSE radiation is from the forward shock. In addition, some of the observed differences between short and long bursts are also explained.

We make the following choices for the values of the fixed parameters:

1. We take  $\epsilon_B = 10^{-2}$  in both the forward and reverse shock. This value is high enough to yield the observed duty cycles and low enough to allow the forward shock emission to fall within the BATSE range for long duration bursts.
2.  $\epsilon_e = 0.5$  in both the forward and reverse shocks. This is in order to make the bursts as efficient as possible.
3.  $\xi = 1$ , i.e., all bursts correspond to the Newtonian regime for the reverse shock. This assumption is merely for simplicity, so that we do not need to worry about a second parameter  $\xi$ , in addition to  $\gamma$ . We expect  $\xi = 1$  to be satisfied if all bursts begin with sufficiently thin shells initially, e.g.,  $\Delta < 10^7$  cm, and spread out so as to be quasi-relativistic.
4.  $l = 10^{18}$  cm,  $n_1 = 1 \text{ cm}^{-3}$ , i.e., all the bursts have the same explosion energy and expand into a standard ISM.

In this model, the distributions of various burst properties are determined by the distribution of  $\gamma$  over the burst population. This distribution could in principle be a complicated function, but we make the simple assumption that  $\gamma$  is distributed uniformly in logarithm from low values of  $\gamma$  up to some upper limit  $\gamma_{\text{max}} \sim 10^4$ . We assume further (again for simplicity) that the bursts originate in a Euclidean space. This is almost certainly wrong, since there is evidence for a considerable cosmological effect in the BATSE data. Nevertheless, the assumption is appropriate for such a crude model. The Euclidean assumption allows us to estimate the number of bursts expected to be detected simply as the detection efficiency to the power of  $3/2$ .

Using the above assumptions, we can calculate the relative numbers of bursts expected to be detected by BATSE as a function of burst duration  $t_{\text{dur}}$ . Each value of  $t_{\text{dur}}$  corresponds to a fixed value of  $\gamma$  (see eq. [3] with  $\xi = 1$  and fixed  $l_{18}$ ). For this  $\gamma$ , we calculate the synchrotron emission as a function of the observed photon energy  $h\nu_{\text{obs}}$  separately for

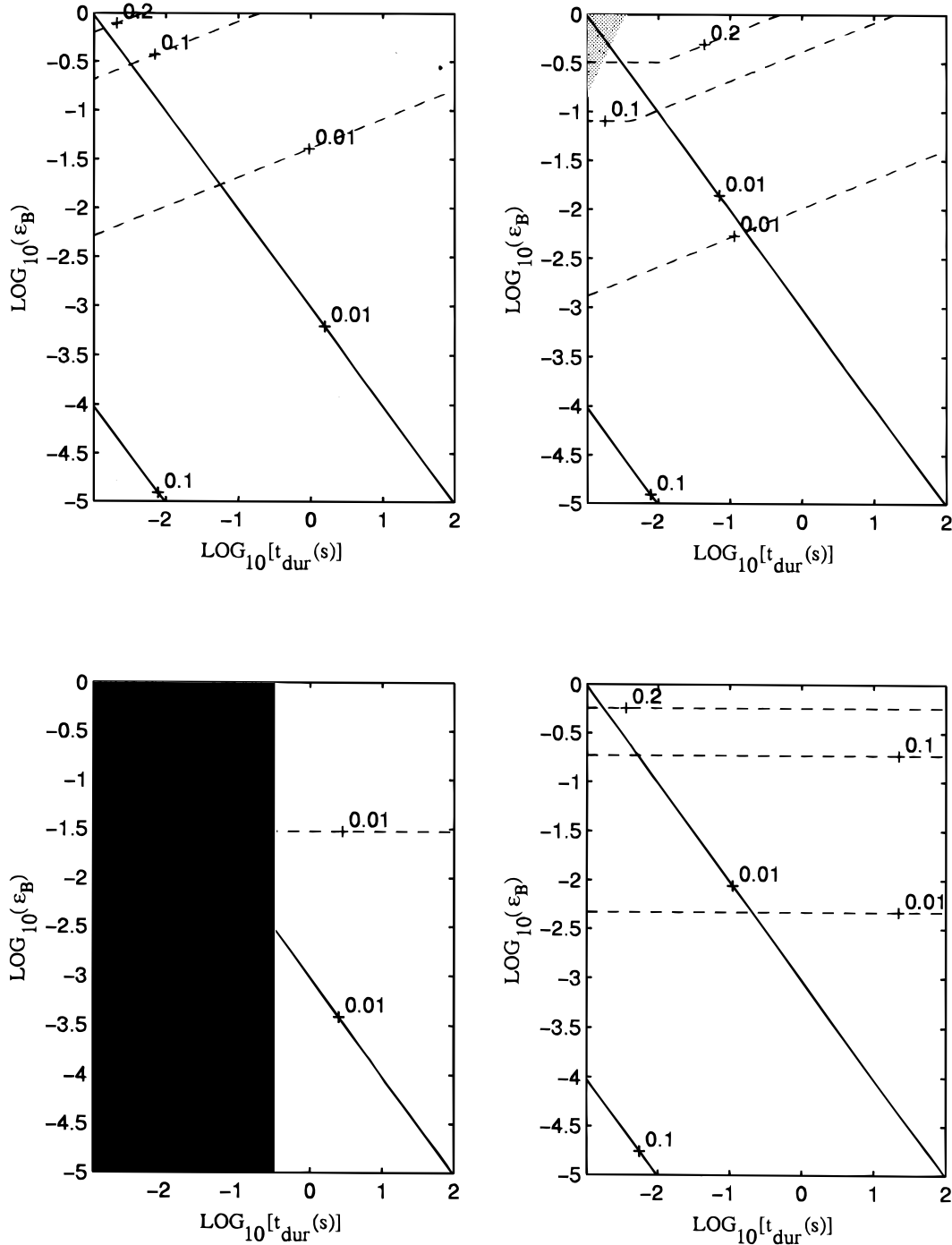


FIG. 5.—Similar to Fig. 4, but for the reverse shock, for  $\epsilon_e = 0.5$ . The four panels are as follows. *Top left*:  $\xi = 1$ ; *top right*:  $\xi = 0.1$ ; *bottom left*:  $\gamma = 10^3$ ; *bottom right*:  $\gamma = 10^4$ . IC cooling is present in all regions and has been included in calculating the durations and efficiencies. The dark region is not physical, since there are no bursts of duration less than 0.3 s with  $\gamma = 10^3$ .

the forward and reverse shock. Then we calculate the photon count rate that BATSE would detect from this burst and take the 3/2 power of this quantity to obtain the relative volume over which BATSE is sensitive to such bursts. We say that the number of bursts expected to be detected is proportional to the volume. Figure 6 shows the calculated distribution of detected bursts as a function of burst duration. The sudden break at  $t_{\text{dur}} \sim 10$  s arises because for shorter bursts the radiation from the forward shock is too hard to fall within the BATSE range.

Although the above calculation gives the main idea, some further details related to BATSE's detection criteria need to

be taken into consideration. BATSE detects a burst if the photon count rate is higher than a limit set by the background. This limit varies depending on the particular trigger used. BATSE's triggers are set by the count rates in three time resolutions: 64 ms, 256 ms, and 1024 ms. The count rate threshold is lower in the 1024 ms channel by a factor of 2 than in the 256 ms channel, and by a factor of 4 compared to the 64 ms channel. Thus, long bursts are detected most sensitively by the 1024 ms channel. On the other hand, short bursts are preferentially detected in the shorter channels because their signals becomes smeared out in the 1024 ms channel. It is straightforward to include this

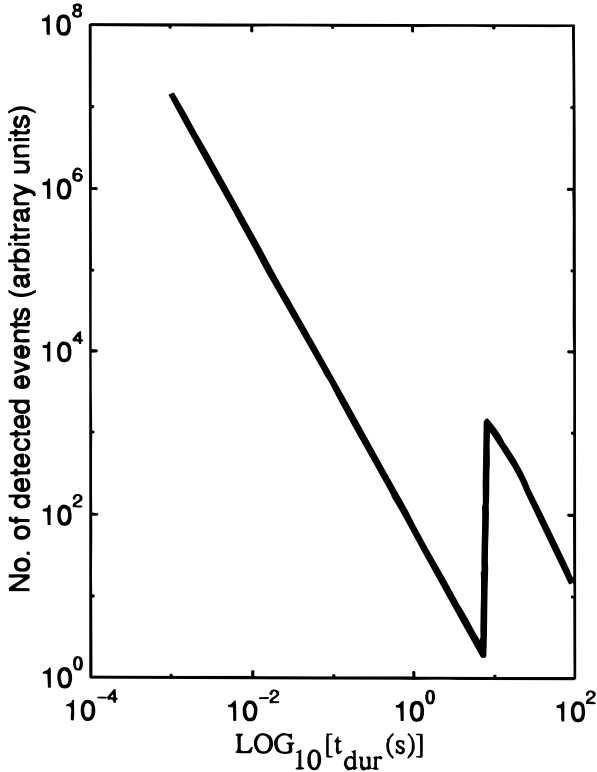


FIG. 6.—The number of bursts expected to be detected by BATSE as a function of burst duration if the distribution of sources is homogeneous and the detection criterion is set solely by luminosity. The calculations correspond to  $\epsilon_e = 0.5$  and  $\epsilon_B = 0.01$ . For the reverse shock, we have taken  $\xi = 1$  (Newtonian shock). The peak on the right corresponds to bursts for which the forward shock is visible to BATSE, while the peak on the left is due to bursts for which only the reverse shock is visible.

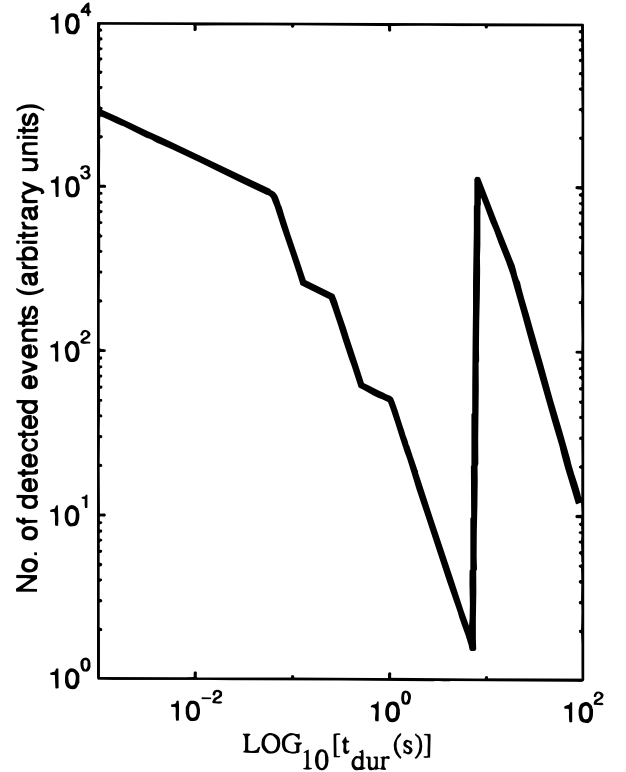


FIG. 7.—Similar to Fig. 6, but including the effect of BATSE's three time channels, 64 ms, 256 ms, and 1024 ms, in calculating the detectability of bursts. Note the bimodal distribution of durations. In this model, short bursts are due to radiation from the reverse shock in fireballs of high  $\gamma$ , while long bursts are due to the emission from the forward shock in low  $\gamma$  fireballs.

selection effect in the model (see Mao et al. 1994). Figure 7 shows the expected distribution of durations of detected bursts with the correction included.

We see that Figure 7 qualitatively resembles the observed distribution of burst durations except for a few differences that are expected and explained below. The model predicts the number of bursts to grow with decreasing duration even below 10 ms, whereas the observed distribution seems to roll over at short durations. This discrepancy is fixed easily if we take the distribution of  $\gamma$  not to be uniform in  $\log \gamma$  but to have fewer bursts with high  $\gamma$  (as is plausible). The model also has an abrupt step at  $t_{\text{dur}} \sim 10$  s caused by the fact that the forward shock is not detected for shorter duration. The step would be rounded off if we do not take the various parameters other than  $\gamma$  to be absolute constants but allowed them some variation. The shape of the peak would change also if we would allow electrons to cool below  $\gamma_{e,\text{min}}$  (see the comment below eq. [23]), but we ignore this effect in the present simplified discussion.

One interesting result of the above exercise is that the bursts in the second peak, the long bursts, have efficiencies close to unity and therefore would correspond to a BATSE-observed luminosity of order  $E \sim 10^{51}$  ergs. However, the short bursts in general have significantly lower efficiencies of order a few percent. Therefore, this model predicts that the short bursts should be less luminous, and therefore that BATSE should detect them out to a shorter distance than the long bursts. Mao et al. (1994) found exactly this effect in the data when they carried out a detailed analysis of the

BATSE sample of bursts. Further, Mao et al. showed that the long and short bursts have similar peak luminosities even though they differ by a factor of 30 in their durations and fluences. Our model does indeed produce similar peak luminosities within the BATSE band for the two classes of bursts. For example, a burst of duration 10 s has the same luminosity as a short burst of 0.2 s, while a burst of duration 2 s, which is too short for the forward shock to be detected, is less luminous by a factor of about 15.

## 8. DISCUSSION

Our basic picture follows the scenario proposed by Mészáros & Rees (1992), namely, that a GRB is produced when a relativistic outflow of particles from a central explosion is slowed down by interaction with an external ISM. The interaction takes place in the form of two shocks—a forward shock that propagates into the ISM and a reverse shock that propagates into the relativistic shell. We have used the results of Sari & Piran (1995) to express the density, velocity, and thermal energy of the gas in the shocked regions in terms of physical parameters such as the Lorentz factor  $\gamma$  of the relativistic flow and the density of the external medium. Some properties of the shocked medium are, however, impossible to estimate from first principles. One such property is the energy density of the magnetic field, which we write as a fraction  $\epsilon_B$  of the total energy. Another is the fraction of the thermal energy that goes into electrons, which we write as  $\epsilon_e$ . We consider  $\epsilon_B$  and  $\epsilon_e$  to be free parameters (though constrained to be less

than unity) that we adjust by comparing the predictions of the model with observations.

We calculate the radiation emitted by the shocked gas via synchrotron emission and also consider modifications introduced by inverse Compton (IC) scattering. In comparing the predictions of the model to observations, we use two important constraints. First, we know that most GRBs have a complex time structure with a duty cycle (defined to be the duration of the sharpest feature divided by the overall duration of the burst) of a few percent. Therefore, we require the cooling time of the shock-heated electrons in our model to be short enough to satisfy this constraint. Second, we impose the requirement that a reasonably large fraction of the shock-generated thermal energy should ultimately be visible as radiation within the BATSE window, 25 keV to 1 MeV. Most proposed models of GRBs have a limited overall energy budget  $\sim 10^{53}$ – $10^{54}$  ergs and convert only a percent or so of this energy into kinetic energy of the expanding shell. If there were any further inefficiency in converting the kinetic energy into BATSE-visible radiation, then it would be very hard to match the observed fluences of GRBs, which correspond to a  $\gamma$ -ray energy output  $\sim 10^{51}$  ergs per burst.

One of the primary results of this paper is that we have calculated the cooling time of the shock-heated electrons via synchrotron emission and IC scattering. We reach several interesting conclusions.

1. For photons detected by BATSE, say of energy 100 keV, there is a very well defined relation between the synchrotron cooling time  $\tau_{\text{syn}}$  of the electrons and the observed duration of a GRB  $t_{\text{dur}}$ . The relation is given in equation (24) and is the same for both the forward and reverse shocks, and it is independent of whether the reverse shock is Newtonian or relativistic. Equation (25) gives a formula for the duty cycle of a burst and predicts that the duty cycle should be nearly independent of burst duration. This prediction appears to be supported by observations but needs to be checked against the data in more detail.

2. If we require the duty cycle to be no more than a few percent, as suggested by the observations, then we find that the magnetic field parameter  $\epsilon_B$  must be greater than about  $10^{-2}$  (assuming  $\epsilon_e \sim 1$ ; see below). Such strong fields are not expected merely from flux freezing, especially in the forward shock in which the field in the external ISM is likely to be very low. We conclude, therefore, that the ultrarelativistic shocks in GRBs must have some mechanism to build up the magnetic field to near-equipartition strength in the postshock gas.

3. We find that the duty cycle should decrease with increasing photon energy as  $(h\nu_{\text{obs}})^{-1/2}$ . Such a variation in widths of features in GRB light curves has been reported by Fenimore et al. (1995). These authors find a variation of the form  $(h\nu_{\text{obs}})^{-0.4}$ , which is reassuringly close to our predicted scaling.

4. IC scattering does not modify the results for the forward shock because the scattering cross section is suppressed strongly by the Klein-Nishina effect. For the reverse shock, IC can be important in some cases. While the IC radiation never falls within the BATSE window, the electrons that produce the BATSE-visible synchrotron radiation can be cooled significantly by IC if  $\epsilon_B < \epsilon_e$ .

In addition to the cooling timescale, we also calculate the efficiency of a burst. The efficiency depends on the param-

eter  $\epsilon_e$ , which determines how much energy is available in the electrons, but also on exactly how much of the energy is actually radiated within the BATSE range. Our analysis leads to the following conclusions.

1. We find that the radiation from the forward shock is visible to BATSE only for bursts with long durations,  $t_{\text{dur}} > 10$  s. In shorter bursts, the radiation from the forward shock is too hard and falls in the MeV range. This implies that there is a population of MeV bursts to which BATSE is insensitive and that may be worth searching for in future missions (see Piran & Narayan 1995).

2. The radiation from the reverse shock falls within the BATSE window for all bursts. However, the amount of radiation received is maximum for very short duration bursts and decreases with increasing burst duration.

3. Combining the above two results, and imposing the requirement of reasonable burst efficiency, we conclude that  $\epsilon_e$  must be large. This means that ultrarelativistic shocks must be able to accelerate electrons almost as effectively as they accelerate ions. For quantitative estimates, we choose  $\epsilon_e = 0.5$ , which corresponds to the shock thermal energy going into ions and electrons in equal amounts. Even with this choice, we find that the reverse shock is fairly inefficient, with efficiencies as low as 1% for  $\epsilon_B = 10^{-2}$  and  $t_{\text{dur}} > 1$  s. If we give up burst efficiency as a criterion, then some of the constraints stated earlier become looser. For instance, it may be possible to accept values of  $\epsilon_B$  as low as  $10^{-5}$  (as in Mészáros et al. 1993).

4. For the particular choice of parameters we favor,  $\epsilon_B = 10^{-2}$ ,  $\epsilon_e = 0.5$ , the model provides a natural explanation for the bimodal distribution of burst durations. Long bursts are produced by the forward shock from fireball shells with somewhat low values of  $\gamma \sim 100$ . These bursts are efficient. Short bursts, on the other hand, are produced by the reverse shock from higher  $\gamma$  events. These are in general much less efficient. The model even explains the curious feature noted by Mao et al. (1994) that the luminosities of short and long bursts are similar even though their fluences differ by a large factor. This results naturally in our model from the different efficiencies of the two shocks.

We conclude with two caveats. First, our model in its present form does not have an explanation for the break seen by BATSE in many GRB spectra at around a few hundred keV. In the present paper, we required merely that the model should be able to produce photons visible to BATSE, and we calculated the properties of these photons and the electrons that produce them. An additional requirement we could have imposed, but did not, is a low-energy cutoff so that the model does not produce an excess of X-ray photons. The forward shock in our model does naturally have a low-energy cutoff, and it is possibly consistent with measured constraints in the X-ray band, but the reverse shock in our model produces too much low-energy radiation. It is possible that IC cooling suppresses the lower energy radiation. To investigate this, the IC interactions will need to be calculated in greater detail than we have done in this paper.

The second point is that we have assumed that the overall duration of a burst  $t_{\text{dur}}$  is given by the hydrodynamic time  $t_{\text{hyd}}$ , and that this time is greater than the cooling time  $t_{\text{cool}}$  of the electrons. We associate the widths of individual features in burst profiles with  $t_{\text{cool}}$ . We find this choice natural. However, it is possible to consider the opposite case in

which  $t_{\text{hyd}} < t_{\text{cool}}$ . In such a scenario, individual spikes in the burst profile would correspond to  $t_{\text{hyd}}$ , and the overall duration of the burst and its complicated time structure would need to be generated by some other mechanism, perhaps time-variable ejections in the original source (e.g., Narayan et al. 1992). One problem with such a model is that the efficiency will be low. The expanding shell slows down on the hydrodynamic time, and so any radiation produced after a time  $t_{\text{hyd}}$  is no longer Lorentz boosted and will therefore arrive over a very much longer time than  $t_{\text{hyd}}$  in the

observer frame. Therefore, only a fraction  $t_{\text{hyd}}/t_{\text{cool}}$  of the emitted radiation will be counted as being part of the GRB, leading to loss of efficiency. On the other hand, the model might be able to explain the low-energy spectral indices of GRBs and the paucity of X-ray photons (Katz 1994).

R. N. and T. P. thank the ITP at USCB for hospitality where this research was begun. This work was supported in part by NASA grant NAG 5-1904, by an NSF grant to ITP, and by an INSF grant to the Hebrew University.

#### REFERENCES

- Band, D., et al. 1993, *ApJ*, 413, 281  
 Bhat, P. N., et al. 1994, in *AIP Conf. Proc.* 307, *Gamma-Ray Bursts*, ed. G. J. Fishman, J. J. Brainerd, & K. Hurley (New York: AIP), 197  
 Cohen, U., & Piran, T. 1995, *ApJ*, 444, L25  
 Fenimore, E. E., et al. 1993, *Nature*, 366, 40  
 ———. 1995, *ApJ*, 448, L101  
 Katz, J. I. 1994, *ApJ*, 432, L107  
 Kouveliotou, C., et al. 1993, *ApJ*, 413, L101  
 Lamb, D. Q., Graziani, C., & Smith, I. A. 1993, *ApJ*, 413, L11  
 Mao, S., Narayan, R., & Piran, T. 1994, *ApJ*, 420, 171  
 Mészáros, P., Laguna, P., & Rees, M. J. 1993, *ApJ*, 415, 181  
 Mészáros, P., & Rees, M. J. 1992, *MNRAS*, 258, 41P  
 Narayan, R., Paczyński, B., & Piran, T. 1992, *ApJ*, 395, L83  
 Piran, T. 1995, in *Some Unsolved Problems in Astrophysics*, ed. J. Bahcall, & J. P. Ostriker (Princeton: Princeton Univ. Press), in press  
 Piran, T., & Narayan, R. 1995, in *AIP Conf. Proc.*, *Gamma-Ray Bursts*, ed. C. Kouveliotou, M. S. Briggs, & G. J. Fishman (New York: AIP), in press  
 Rybicki, G. B., & Lightman, A. P. 1979, *Radiative Processes in Astrophysics* (New York: Wiley)  
 Sari, R., & Piran, T. 1995, *ApJ*, 455, L143 (SP)  
 Thompson, C. 1994, *MNRAS*, 270, 480  
 Woosley, S. E. 1993, *ApJ*, 405, 273